DEVELOPMENTAL DYNAMICS 214:13–25 (1999)

Analysis of a Zebrafish Semaphorin Reveals Potential Functions In Vivo

MARY C. HALLORAN,[1] SHAWN M. SEVERANCE,[1] CHARLES S. YEE,[1] DEBRA L. GEMZA,[1] JONATHAN A. RAPER,[2] AND JOHN Y. KUWADA[1]*
[1]*Department of Biology, University of Michigan, Ann Arbor, Michigan*
[2]*Department of Neuroscience, University of Pennsylvania School of Medicine, Philadelphia, Pennsylvania*

ABSTRACT **The semaphorin/collapsin gene family is a large and diverse family encoding both secreted and transmembrane proteins, some of which are thought to act as repulsive axon guidance molecules. However, the function of most semaphorins is still unknown. We have cloned and characterized several semaphorins in the zebrafish in order to assess their *in vivo* function. Zebrafish *semaZ2* is expressed in a dynamic and restricted pattern during the period of axon outgrowth that indicates potential roles in the guidance of several axon pathways. Analysis of mutant zebrafish with reduced *semaZ2* expression reveals axon pathfinding errors that implicate SemaZ2 in normal guidance. *Dev Dyn 1999;214: 13–25.*** © 1999 Wiley-Liss, Inc.

Key words: axon guidance; semaphorin; collapsin; zebrafish

INTRODUCTION

As the nervous system develops, axons navigate along specific pathways by following guidance cues located in precise locations of their environment. These guidance cues can be either attractive or repulsive to the axon's growth cone. Recently, the search for molecules capable of guiding growth cones has led to the identification of several gene families encoding proteins thought to act as axon guidance molecules (reviewed in Culotti and Kolodkin, 1996; Tessier-Lavigne and Goodman, 1996). The semaphorin/collapsin gene family is a large and diverse family encoding both secreted and transmembrane proteins, some of which are repulsive axon guidance molecules. Semaphorins have a characteristic extracellular sema domain of approximately 500 amino acids, and are grouped into six classes based on other structural domains of the proteins they encode (Adams et al., 1996; Kolodkin, 1996; Zhou et al., 1997). To date, numerous semaphorins have been identified in humans (Kolodkin et al., 1993; Hall et al., 1996; Roche et al., 1996; Sekido et al., 1996; Xiang et al., 1996), rodents (Inagaki et al., 1995; Püschel et al., 1995; Adams et al., 1996; Furuyama et al., 1996; Giger et al., 1996; Eckhardt et al., 1997; Kikuchi et al., 1997; Zhou et al., 1997; Christensen et al., 1998), chick (Luo et al.,1993, 1995), and insects (Kolodkin et al., 1993). In addition, analysis of the human EST database indicates that the number of semaphorins in the vertebrate genome may exceed 20.

The evidence that semaphorins may act as axon guidance molecules has come from a number of in vitro and in vivo studies. The first vertebrate semaphorin identified, chick Collapsin-1 (Coll-1) (Luo et al., 1993), and its mammalian homologs SemaD/III (Kolodkin et al., 1993; Püschel et al., 1995), can inhibit specifically the outgrowth of particular spinal and cranial sensory and motor axons (Püschel et al., 1995, 1996; Messersmith et al., 1995; Kobayashi et al., 1997; Shepherd et al., 1997; Varela-Echavarria et al., 1997), suggesting it normally acts to guide these axons. In support of this hypothesis, mice lacking the *semaIII/D* gene show defects in the outgrowth and pathfinding of spinal sensory and cranial nerve axons (Behar et al., 1996; Taniguchi et al., 1997). Analyses of the in vivo function of semaphorins in *Drosophila* and grasshopper have shown that the transmembrane semaphorin SemaI may have a dual role in axon guidance, acting as an attractive/permissive cue for some axons, and a repulsive cue for others (Kolodkin et al., 1992; Wong et al., 1997; Yu et al., 1998). Moreover, a role for *Drosophila* SemaII in directing an axon's choice of synaptic target has been demonstrated by experiments in which SemaII expression levels were perturbed on target muscle fibers (Matthes et al., 1995; Winberg et al., 1998).

Increasing evidence indicates that semaphorins function not only in axon guidance and synapse formation but also in a broad range of developmental processes. One mouse *semaIII* knockout line displays defects in bone and cartilage formation as well as excessive growth of the heart, suggesting that SemaIII may function to restrict growth of these tissues during development (Behar et al., 1996). Interestingly, two human semaphorin genes, *semaIV* and *semaV*, were

Grant sponsor: NINDS; Grant number: NS36587; Grant sponsor: APA; Grant numbers: KAI-9603 and KAR1–9704; Grant sponsor: NRSA; Grant number: NS09877–01; Grant sponsor: National Institutes of Health; Grant number: M01RR00042.

Charles S. Yee's present address is Department of Surgery, Children's Hospital, 300 Longwood Avenue, Boston, MA 02115.

*Correspondence to: John Y. Kuwada, Department of Biology, University of Michigan, Ann Arbor, MI 48109–1048. E-mail: kuwada@umich.edu

Received 24 July 1998; Accepted 18 September 1998

isolated from a chromosomal region that is deleted in several lung cancers, suggesting that these semaphorins may possess tumor suppressant activity and/or may function in normal lung development (Roche et al., 1996; Sekido et al., 1996; Xiang et al., 1996). In addition, a role for semaphorins in immune system function has recently been demonstrated. The gene encoding a leukocyte activation antigen, human CD100, was cloned and determined to be a transmembrane member of the semaphorin family (Hall et al., 1996). These studies show that semaphorins may act as signaling molecules with widespread functions including regulation of cell movements, cell differentiation, and tissue modeling. Our understanding of how the combined action of the large number of semaphorins contributes to development is far from complete, as the in vivo function of most family members has yet to be determined.

In order to analyze the in vivo function of semaphorins during development of the vertebrate nervous system, we initiated the cloning and analysis of zebrafish semaphorins. The zebrafish has several characteristics advantageous for investigation of semaphorin gene function during development. Embryos are transparent, develop rapidly, and are accessible at all stages of development. The axonal pathways of the nervous system are established by a relatively small number of identified neurons whose individual trajectories are well characterized (Eisen et al., 1986; Mendelson, 1986; Myers et al., 1986; Bernhardt et al., 1990; Chitnis and Kuwada, 1990; Kuwada et al., 1990a,b; Wilson et al., 1990; Ross et al., 1992). A potential zebrafish homolog to *coll-1* and *semaD/III*, *semaZ1a*, as well as two novel semaphorins, *semaZ7* and *semaZ8*, have previously been identified (Yee et al., 1995; Halloran et al., 1998). Like Coll-1, SemaZ1a can cause collapse of chick DRG growth cones in vitro, suggesting it may share in vivo functions with Coll-1. Manipulation of *semaZ1a* expression in vivo has demonstrated that SemaZ1a likely plays a role in guiding the sensory axons of the zebrafish lateral line (Shoji et al., 1998). We have now identified several more semaphorin family members in the zebrafish. The developmental expression pattern of one of these, *semaZ2*, suggests it functions to guide the formation of several axon pathways, and alterations in *semaZ2* expression in mutant zebrafish lines correlate with errors in the pathfinding of predicted axons.

RESULTS

Cloning Of Zebrafish Members Of The *Semaphorin* Gene Family

To identify *semaZ2*, we screened a zebrafish embryonic cDNA library at reduced stringency with a probe complementary to chick *collapsin-1*. Weakly hybridizing plaques were purified further by hybridization at reduced stringency to the zebrafish semaphorin, *semaZ1a*. One phage insert was a 2.5 kb cDNA with an open reading frame lacking only the sequence 5' to the sema domain, and showed strong sequence similarity to chick *collapsin-2* (Luo et al., 1995). We obtained the entire coding sequence for *semaZ2* by using rapid amplification of cDNA ends (5'-RACE), and ligated the RACE PCR product to the 2.5 kb cDNA to generate a 2.9 kb cDNA containing a complete open reading frame.

The cDNA sequence for *semaZ2* predicts a protein of 764 amino acids with structure similar to other semaphorins (Fig. 1A). The amino-terminal region shows characteristics of a signal sequence with a predicted signal peptide cleavage site at amino acid 42. Because the remainder of the sequence contains no potential transmembrane domain, the protein is likely secreted. The deduced amino acid sequence contains four potential sites for N-linked glycosylation and 19 cysteine residues conserved between SemaZ2 and chick Collapsin-2 (Coll-2), including the 13 cysteines conserved among all vertebrate sema domains. SemaZ2 has the same structural domains as the semaphorins of class III and shares the highest sequence identity with chick Coll-2 (64% amino acid identity over the entire coding region). The sema domain of SemaZ2 shares 71% amino acid identity with that of Coll-2, and is followed by a single immunoglobulin-like (Ig) domain with 62% amino acid identity to Coll-2. SemaZ2 also has a highly basic carboxy terminal region sharing 72% amino acid identity with Coll-2. The degree of amino acid identity between SemaZ2 and Coll-2 is markedly higher than between SemaZ2 and all other semaphorins, including the most closely related zebrafish semaphorin, SemaZ1a, suggesting that SemaZ2 may be a zebrafish homolog to Coll-2 (Table 1).

In parallel experiments, we used a PCR-based approach to search for zebrafish genes with sequence similarity to chick collapsins. We used degenerate oligonucleotide primers to conserved regions of the sema domain to amplify cDNA sequences from total RNA of zebrafish embryos at 24 hr post-fertilization (hpf). We obtained five different PCR products of the expected length (0.8 kb). Sequence analysis revealed that these semaphorin fragments encode partial open reading frames covering the carboxy half of the sema domain of five different zebrafish semaphorins (Fig. 1B). The nucleotide sequence of one of these was identical to the corresponding portion of the *semaZ2* cDNA. The other four, however, proved to be novel sequences different from *semaZ1a*, *Z2*, *Z7*, and *Z8*. One of the four has sequence most similar to Coll-1/SemaD/III (86% amino acid identity) and SemaZ1a (84% identity), and has considerably lower similarity to all other semaphorins (Table 1). This sema fragment is in fact identical in sequence to another recently identified zebrafish semaphorin, SemaZ1b (Marc Roos, Robert Bernhardt, and Melitta Schachner, personal communication), which is another candidate zebrafish homolog to Coll-1/SemaD/III. We have named the remaining three partial semaphorins *semaZ9–11* until their complete sequences are obtained and they can be defini-

A

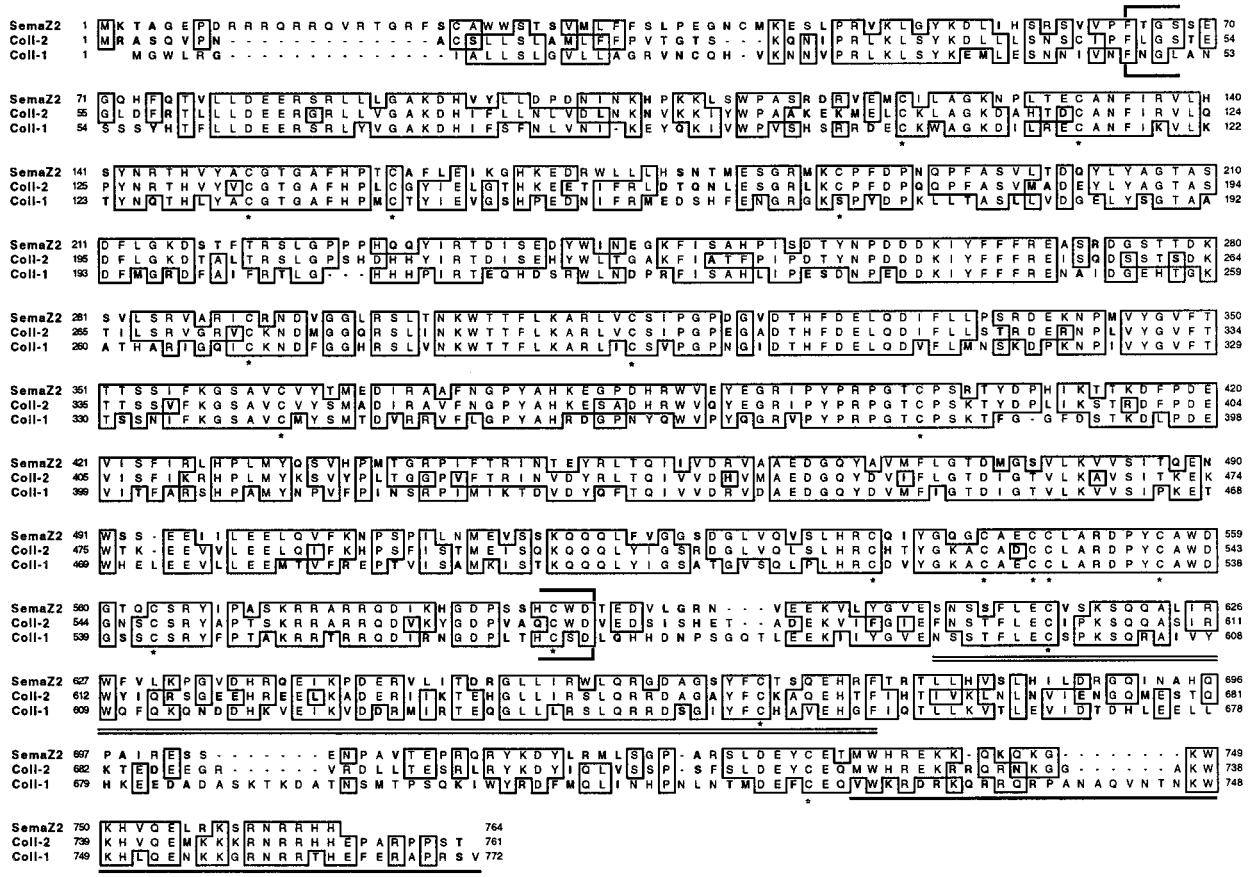

B

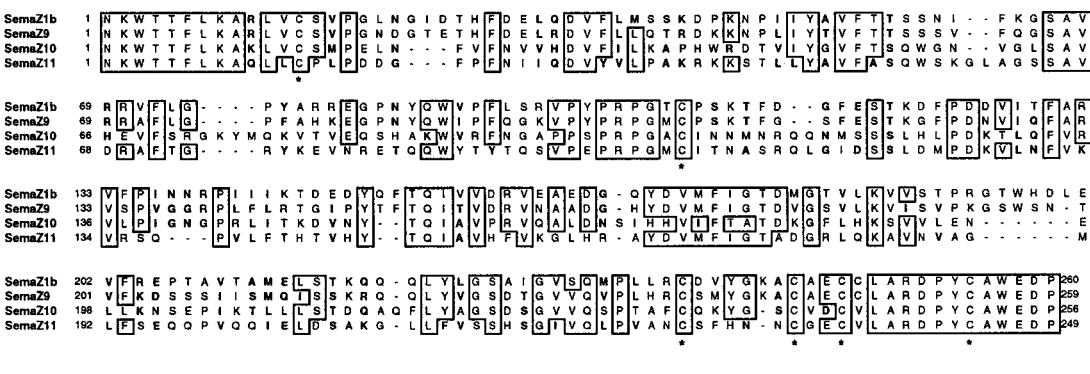

Fig. 1. **A:** Comparison of the sequences of SemaZ2 with related chick collapsins Coll-1 and Coll-2. Alignments of predicted amino acid sequences were generated with the MacVector ClustalW alignment program. Identical amino acids are boxed and similar amino acids are shown in bold. Brackets delineate the sema domain, double underline denotes the Ig domain, and single underline denotes the basic carboxy terminus. Asterisks mark conserved cysteine residues. **B:** Alignment of the predicted amino acid sequences of the semaphorin fragments SemaZ1b and SemaZ9-Z11. Alignment was generated with the MacVector ClustalW alignment program. Identical amino acids are boxed and similar amino acids are shown in bold. Asterisks denote conserved cysteine residues.

TABLE 1. Percentage Amino Acid Identity Within the Sema Domain

	Sema Z2	Sema Z1b	Sema Z9	Sema Z10	Sema Z11
CLASS III					
SemaZ1a	55.8	84.5	66.7	41.4	38.4
SemaZ2	—	62.2	63.6	39.2	36.0
SemaZ8[a]	52.2	58.2	57.3	40.0	35.8
C-Coll-1	57.7	86.4	67.4	41.4	38.4
C-Coll-2	71.5	62.2	60.9	40.4	36.0
C-Coll-3	51.3	55.9	60.9	39.6	32.7
C-Coll-5	51.0	58.9	59.7	37.4	33.0
M-SemD	57.3	86.4	67.1	42.9	39.2
M-SemA	54.0	64.0	74.4	38.1	38.6
M-SemE	52.3	57.1	62.4	39.7	34.4
H-SemaIII	58.4	85.7	67.1	42.5	38.4
H-SemaIV	50.9	59.8	65.1	39.2	34.9
H-SemaV	55.8	64.0	74.0	37.7	38.2
CLASS IV					
SemaZ7	36.7	36.5	38.5	45.1	42.1
M-SemB	33.8	32.8	33.7	41.1	46.4
M-SemC	34.9	33.6	36.8	44.9	59.9
M-SemaG[b]	38.2	43.4	40.8	63.2	47.5
M-SemaF[b]	36.2	38.7	38.4	47.2	43.8
H-CD100	38.0	41.4	39.7	62.5	45.3

[a]Amino acid identities for SemaZ8 are within its partial sema domain.
[b]M-SemaF and M-SemaG are those cloned by Inagaki et al. (1995) and Furuyama et al. (1996).

tively categorized. Based on amino acid identity to other semaphorins within this partial sema domain, SemaZ9 is likely a class III semaphorin. It shows the greatest sequence similarity to mouse SemA (Püschel et al., 1995) and human SemaV (Sekido et al., 1996) (74% amino acid identity), with slightly lower identities (59–67%) to other class III semaphorins (Table 1). In contrast, the amino acid sequences of SemaZ10 and Z11 within the partial sema domain suggest they are likely class IV semaphorins (Table 1). SemaZ10 shares the highest sequence identity with M-Sema G (Furuyama et al., 1996) (63%) and shows lower identities with other members of class IV, including zebrafish SemaZ7 with which it shares 45% identity. SemaZ11, also of class IV, is most similar to mouse SemC (Püschel et al., 1995) (60% amino acid identity) and shows much lower similarity to other semaphorins.

semaZ2 mRNA Is Expressed in the Developing Central Nervous System

We performed whole mount in situ hybridization with digoxigenin labeled *semaZ2* antisense riboprobes to examine the distribution of *semaZ2* transcripts from 12 to 72 hpf, when much of nervous system development is occurring. We found *semaZ2* mRNA expression in a number of neuroectodermal and mesodermal tissues during these stages of development. *semaZ2* sense riboprobes showed no detectable hybridization at any stage.

Forebrain/midbrain. By 16 hpf in the zebrafish, the major brain divisions can be distinguished and the first neurons are beginning to extend axons in the brain. No expression of *semaZ2* mRNA was detected in the telencephalon at any age examined. However, beginning at 16 hpf and continuing at least through the second day of development, *semaZ2* mRNA is expressed in two regions of the diencephalon (Fig. 2A–F). One expression domain is located in the rostral most diencephalon, spanning the midline at the base of the optic stalks. The second domain covers the width of the neuroepithelium at the caudoventral diencephalon and may extend into the midbrain tegmentum.

Because semaphorins are thought to influence growing axons, we examined the relationship between these *semaZ2* expressing cells and the early developing axonal pathways in the diencephalon. Axons were labeled with an antibody to acetylated tubulin in embryos that had previously been processed for *in situ* hybridization to *semaZ2* (Fig. 2D,E). The axons that form the initial scaffold of tracts in the brain for the most part grow around but not through the domains of *semaZ2* expression, suggesting SemaZ2 may act as an inhibitory guidance molecule. In particular, axons of the nucleus

Fig. 2. Developmental expression pattern of *semaZ2* in the diencephalon and hindbrain. Whole mount in situ hybridization for *semaZ2* mRNA. Unless otherwise noted, embryos are oriented with rostral to the left and dorsal up. **A:** Lateral view of whole embryo at 25 hpf showing *semaZ2* mRNA expression in blue. **B:** Ventral view of 24 hpf forebrain showing two regions of *semaZ2* expression in the diencephalon (white asterisks in B–F denote the two domains of expression in diencephalon). **C:** Lateral view of diencephalon expression at 25 hpf. **D:** Lateral view of double labeled brain at 25 hpf. *In situ* hybridization for *semaZ2* is in blue and antibody against tubulin labeling axon tracts is in brown. **E:** Higher magnification view of epiphysial axons in the DVDT and axons of the nucPC extending on either side of *semaZ2* expression. **F:** Ventral view of diencephalon at 50 hpf. Arrowheads delineate the location of retinal axons crossing the midline in the optic chiasm between the domains of *semaZ2* expression. **G:** Transverse section through midbrain of 36 hpf embryo showing *semaZ2* expression in optic tectum. Arrowheads delineate dorsal and ventral borders of one optic lobe. **H:** Dorsal view of 12 hpf embryo showing *semaZ2* expression in rhombomeres 3 and 5 and in the notochord. **I:** Lateral view of 15 hpf embryo showing hindbrain *semaZ2* expression. Arrowheads delineate gap in floor plate expression. **J:** Lateral view of 16 hpf embryo showing hindbrain rhombomeres 3, 4, and 5. Expression of *krox20* is in red and expression of *semaZ2* is in blue. Arrowhead indicates break in floor plate *semaZ2* expression at the rostral limit of the notochord. **K:** Lateral view of 18 hpf embryo showing hindbrain region. Asterisk labels neural crest cells out of the plane of focus (see Fig. 6). Arrowheads delineate gap in floor plate expression. **L:** Lateral view of 24 hpf embryo. *semaZ2* expression in floor plate is restricted to a few cells at the caudal hindbrain at this age. Expression is also present in the roof plate of the spinal cord. **M:** Lateral view of hindbrain of 36 hpf embryo. *semaZ2* is expressed in dorsal clusters in the rhombomere boundary regions and in a ventral domain in r4. **N:** Dorsal view of hindbrain of 36 hpf embryo showing *semaZ2* expressing clusters at rhombomere boundaries and across the midline of rhombomere 4. **O:** Transverse cryostat section through rhombomere 4 from a 36 hpf embryo showing location within the hindbrain of *semaZ2* expressing cells. AC, anterior commissure; DVDT, dorsal ventral diencephalic tract; fp, floor plate; hb, hindbrain; mb, midbrain; noto, notochord; PC, posterior commissure; POC, post optic commissure; r3, r4, r5, rhombomeres 3, 4, and 5; rp, roof plate; sc, spinal cord; TPOC, tract of the post optic commissure; TT, telencephalic tract. Scale bars = 100 μm (A–D,F,H–N) and 50μm (E,G,O).

of the posterior commissure (nucPC) located dorsally in the caudal diencephalon initially extend ventrally and then turn caudally away from the *semaZ2* expressing cells upon reaching the ventral diencephalon. Likewise, the epiphysial neurons, which lie in the dorsal diencephalon, extend their axons ventrally, pioneering the

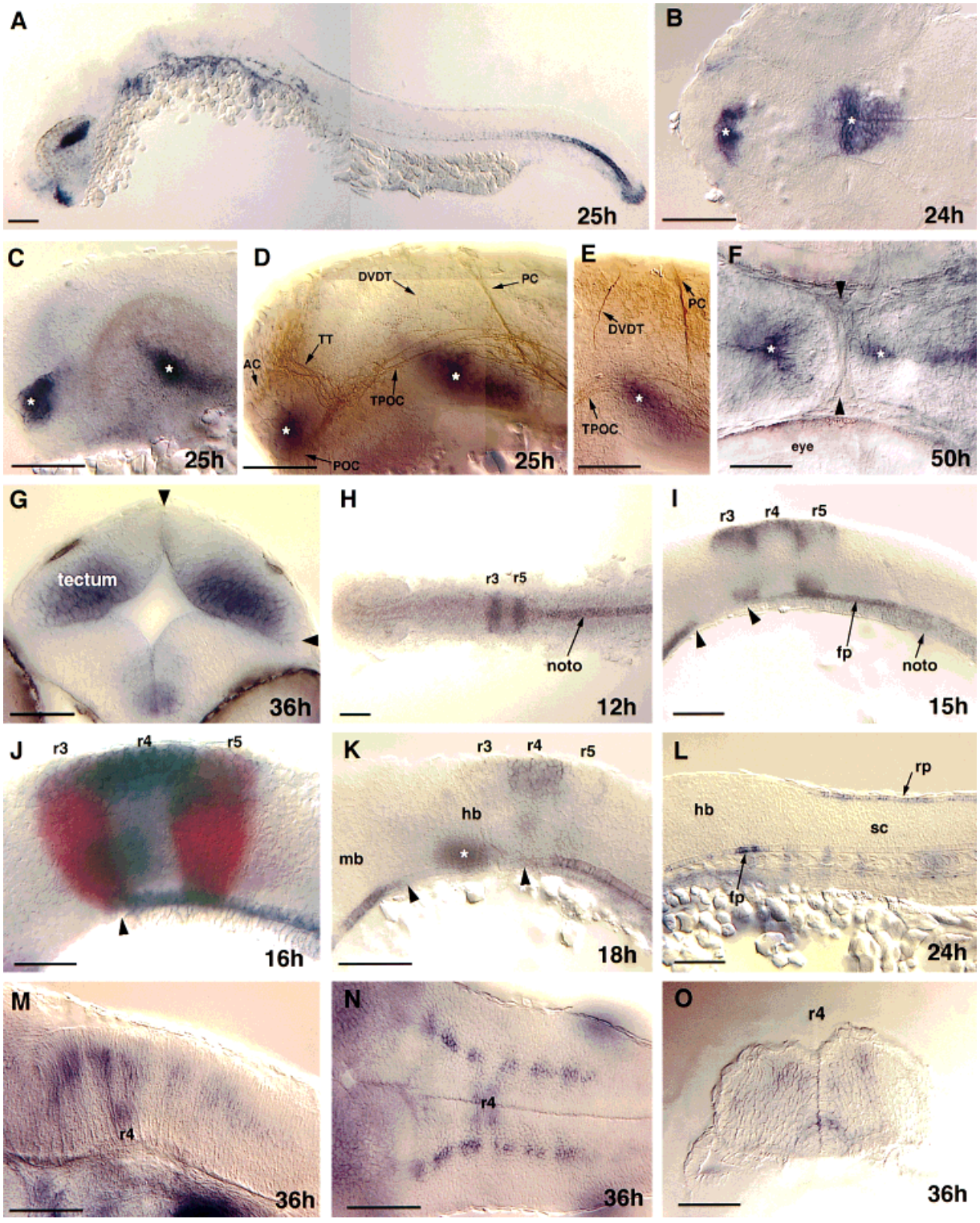

Figure 2.

dorso-ventral diencephalic tract (DVDT) and then turn rostrally away from the *semaZ2* expressing cells (see Fig. 5A for schematic). In the rostral diencephalon, two commissures, the anterior commissure (AC) and the postoptic commissure (POC), cross the midline dorsally and ventrally, respectively, to *semaZ2* expression. Later, retinal ganglion axons extending toward the contralateral optic tectum form the optic chiasm in the ventral diencephalon. These axons cross the midline in a small region located between the two domains of *semaZ2* expression (Fig. 2F). SemaZ2 could potentially act to restrict the growth of retinal axons rostrally and caudally, thus forcing them to grow across to the contralateral diencephalon. At the time retinal axons approach and grow into the optic tectum, *semaZ2* is expressed only in the ventral and not dorsal tectum (Fig. 2G), suggesting it could function to restrict the growth of retinal axons that innervate the dorsal most tectum.

Hindbrain/spinal cord. In the developing hindbrain, *semaZ2* mRNA exhibits a dynamic pattern of expression during the stages examined. *semaZ2* expression can be detected beginning at 12 hpf in a subset of hindbrain rhombomeres (Fig. 2H–K). Double in situ hybridization with probes to *semaZ2* and to *krox-20*, a gene expressed specifically in rhombomeres 3 and 5 (r3 and r5, Oxtoby and Jowett, 1993), shows that the *semaZ2* expression is restricted to rhombomeres 3, 4, and 5 (Fig. 2J). At 12 hpf, *semaZ2* expression is seen only in r3 and r5 (Fig. 2H). By 15 hpf, expression in r3 and r5 is visible in both a dorsal and ventral domain, with lower expression levels detectable in the dorsal most region of r4 (Fig. 2I). By 18 hpf, the expression in r3 and r5 has decreased, while expression in r4 has increased (Fig. 2K). *semaZ2* expression in r4 continues until at least 36 hpf.

During the time period when the first axons are beginning to extend in the hindbrain (16–20 hpf), *semaZ2* transcripts are detected in an unusual pattern in the floor plate cells at the ventral midline of the CNS. *semaZ2* is expressed in the floor plate cells of the mesencephalon and of the caudal hindbrain rhombomeres r4–r7 (Fig. 2I–K). However, no expression is present in the floor plate of the rostral hindbrain rhombomeres r1–r3, or in the floor plate of the spinal cord. By 24 hpf, only a small group of floor plate cells at the region of the caudal hindbrain/rostral spinal cord are still expressing *semaZ2* (Fig. 2L). The only cells in the spinal cord that do express *semaZ2* mRNA are the single row of roof plate cells at the dorsal midline (Fig. 2L).

By 36 hpf, when the initial axon scaffolding has been established and many later growing axon tracts are still forming, *semaZ2* displays a segmental expression pattern that reflects the hindbrain rhombomeres (Fig. 2M–O). Bilateral clusters of *semaZ2* expressing cells are present dorsally at each rhombomere boundary region. The identity of these cells is not known; they lie in a position medial to the clusters of commissural neurons also present in rhombomere boundary regions (Trevarrow et al., 1990). Expression of *semaZ2* in r4 has persisted, although it is now present only in the ventral aspect of the rhombomere, spanning the ventral midline.

semaZ2 mRNA Is Expressed in Neural Crest, Pharyngeal Arches, and Placodal Derivatives

In the zebrafish, the cranial neural crest arises as distinct masses of cells lying lateral to the neural keel at the level of the midbrain and hindbrain (Schilling and Kimmel, 1994). These cells begin migrating at 15–16 hpf, moving ventrally to populate the pharyngeal arches, which are the primordia of the jaw structures and gills. *semaZ2* is expressed in a subset of cranial neural crest from the onset of migration. At 14 hpf, a cluster of *semaZ2* expressing cells can be seen lateral to rhombomeres 3 and 4 (Fig. 3A). Cell lineage experiments have shown that neural crest cells from this region populate predominantly the second (hyoid) pharyngeal arch, although they can contribute to the first (mandibular) arch as well (Schilling and Kimmel, 1994). By 16–18 hpf, this mass of cells is larger and has migrated rostrally and ventrally (Fig. 3B). Neural crest cells lying caudal to the otic vesicle, which populate the gill arches, begin expressing *semaZ2* by about 20 hpf. Between 20–24 hpf, three clusters of *semaZ2* expressing cells are present in the region of the pharyngeal arch primordia (Fig. 3C). Later, as the arches develop further (36–72 hpf), the expression of *semaZ2* is localized to a subset of cells in each arch mesenchyme (Fig. 3D–F). At 72 hpf, the cartilage and muscle cells of the pharyngeal arches can be recognized by their characteristic morphologies: the muscle striations are visible, and cartilage cells show a distinct cobblestone-like appearance. At this stage, *semaZ2* expression is present in a small group of distal arch cells that do not appear to be either differentiated cartilage or muscle based on these morphologies (Fig. 3F). In addition to the *semaZ2* expression in cranial neural crest, transcripts are also detected in small clusters of cells along the medial surface of each somite. These cells are in the position of trunk neural crest migrating along their medial migration pathway (Fig. 3G).

semaZ2 expression is also detectable in several placodal structures: the nasal placode, the otic placode, and the migrating primordium of the lateral line. Between 22 to 36 hpf, *semaZ2* expressing cells are present at the medial aspect of the nasal pit, at its interface with the telencephalon (Fig. 3H). In the otic vesicle, two small spots of *semaZ2* expression can be seen at 2 days of development (Fig. 3E). These expressing cells lie in the positions of the developing sensory maculae, and may correspond to these sensory patches. The zebrafish posterior lateral line sensory neuromasts develop in part from a placodally derived migrating primordium that moves caudally along the embryo, depositing cells that will differentiate into neuromasts. At 20 hpf, *semaZ2* is expressed in the region caudal to the otic vesicle where the placode initially forms, and later by

the cells in the leading half (caudal half) of the migrating primordium as it progresses along the trunk (Fig. 3I).

semaZ2 Is Expressed in the Notochord, Pectoral Fin Bud, and Tail Bud

semaZ2 mRNA is expressed in the notochord from its earliest stages of development. Initially, from 12–18 hpf, expression is seen throughout the notochord (Fig. 2H,I). Between 18 to 24 hpf, expression is downregulated in a rostral to caudal wave such that only the caudal most notochord is still expressing *semaZ2* by 24 hpf (Fig. 3L). At this stage *semaZ2* transcripts are also detectable in the underlying hypocord.

The pectoral fin bud initiates as an area of condensing mesenchyme lateral to somites 2–3 at 26 hpf. Weak *semaZ2* expression is present from early fin bud formation. By 36–50 hpf, *semaZ2* mRNA is strongly expressed throughout the developing cartilage of the fin bud (Fig. 3J). After 72 hpf, when the fin has developed a broadened fin blade with cartilaginous actinotrichia supports (Kimmel et al., 1995), *semaZ2* expression continues, although it is now restricted to the most distal differentiating cartilage cells (Fig. 3K). Expression of *semaZ2* in the fin bud occurs during the stages that motor axons are extending toward and innervating the fin bud, suggesting SemaZ2 could play a role in defining domains of motor innervation into the fin, perhaps preventing axons from innervating cartilage.

Expression of *semaZ2* mRNA is also detected in the developing tail bud throughout the embryonic stages examined (Fig. 3L).

Altered *semaZ2* Expression in Zebrafish Mutants Correlates With Axon Pathfinding Errors

We analyzed mutant lines of zebrafish to search for alterations in *semaZ2* expression and to determine whether the alterations could be correlated with errors in axon pathfinding. In the mutant *cyclops* (*cyc*), ventral midline structures of the nervous system at all axial levels are missing (Hatta et al., 1991). The two domains of *semaZ2* expression in the diencephalon are completely absent in *cyc* embryos (Fig. 4A,B), as is the expression in the floor plate of the midbrain and hindbrain (Fig. 4C,D). In contrast, other aspects of *semaZ2* expression are normal. Previous work has demonstrated errors in axon pathfinding in *cyc* that could arise from the absence of an inhibitory guidance cue in these regions of normal *semaZ2* expression. For example, epiphysial axons initially extend normally along their ventral trajectory in *cyc*; however they make pathfinding errors at the ventral diencephalon (Patel et al., 1994). In each case, the growth cones failed to turn rostrally, rather they turned caudally or continued ventrally to cross the other side. The pathways followed by the epiphysial growth cones in *cyc* embryos are consistent with the loss of a signal that normally renders the caudal direction unattractive. In the hindbrain of *cyc* embryos, axons also make errors at the ventral midline. Normally, axons of some hindbrain reticulospinal neurons extend toward the ventral midline in the region of *semaZ2* floor plate expression, and then turn and descend ipsilaterally, without crossing the midline. In *cyc*, these axons sometimes inappropriately cross the midline, consistent with the loss of an inhibitory signal in the floor plate (Hatta et al., 1992).

Another zebrafish mutant, *whitetail* (*wit*), also shows altered *semaZ2* expression and corresponding axon pathfinding errors. In *wit*, neurogenesis is affected with embryos displaying increased numbers of early differentiating neurons (Jiang et al., 1996). The expression of *semaZ2* in the diencephalon of *wit* embryos is dramatically reduced (Fig. 4E,F). As in *cyc*, this reduction in *semaZ2* expression is correlated with errors in epiphysial axon navigation. We found epiphysial axons in *wit* embryos that diverge from the normal DVDT pathway and extend inappropriately in the caudal direction (Fig. 4F). This type of error was found in 74% of *wit* embryos (n=23), while only 4% of wild-type embryos (n=23) displayed such errors. In addition to reduced expression in the diencephalon, *semaZ2* expression is completely absent from the spinal cord roof plate of *wit* embryos (Fig. 4G,H). Interestingly, this lack of *semaZ2* expression is again associated with aberrant axon trajectories. The peripheral axons of the Rohon-Beard (RB) sensory neurons extend from cell bodies in the dorsal spinal cord and arborize in the skin. These axons normally innervate only one side of the embryo and do not cross the dorsal midline (Fig. 4I). In *wit* embryos, RB peripheral axons freely cross the dorsal midline and extend over the skin on both sides of the embryo (Fig. 4J).

DISCUSSION

We have identified several new zebrafish members of the semaphorin family. One of the sema fragments we isolated is identical in sequence to *semaZ1b*, a recently cloned potential zebrafish homolog to Coll-1/SemaD/III (Marc Roos, Robert Bernhardt, and Melitta Schachner, personal communication). The other three sema fragments, *semaZ9–11*, do not have strikingly high sequence identity to other vertebrate semaphorins. Until their complete sequence and domain structure is obtained, it is not possible to determine whether they represent novel semaphorins or are homologs to those previously described. *semaZ2* is potentially a zebrafish homolog to chick *coll-2*. These two genes share some common aspects of their expression patterns; both are expressed in the notochord, fin/limb buds, and optic tectum (Luo et al., 1995). However, there are also significant differences in their expression, most notably in the spinal cord, where *coll-2* is expressed in the floor plate, motor neuron pools, and in much of the dorsal spinal cord with the exception of the roof plate. In contrast, *semaZ2* is expressed only in the spinal cord roof plate. Because the functions of *coll-2* and *semaZ2* are not yet known, it is not clear whether these two genes share a common function. It is possible that the function of *coll-2* is served by more than one gene in the

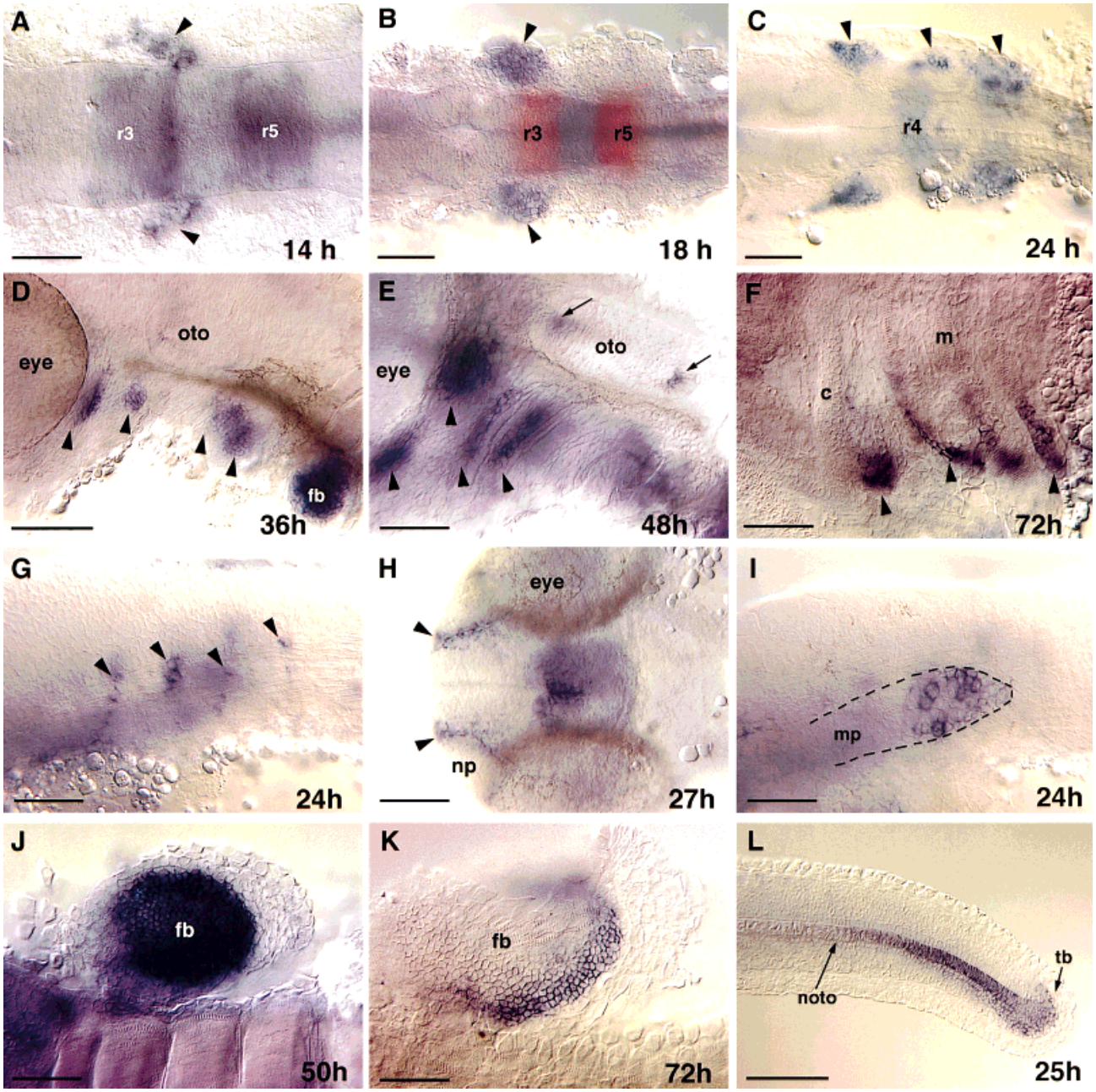

Fig. 3. Whole mount in situ hybridization showing developmental expression pattern of *semaZ2* in the neural crest, pharyngeal arches, and placodal derivatives. **A:** Dorsal view of a 14 hpf hindbrain. Clusters of *semaZ2* expressing cells in the position of neural crest cells are indicated with arrowheads. Expression of *semaZ2* is also present in r3 and r5 at this age. **B:** Dorsal view of 18 hpf hindbrain. Clusters of *semaZ2* expressing neural crest (arrowheads) have increased in size and migrated further rostral and ventral. Rhombomeres 3 and 5 are labeled in red with a probe for *krox20*, and *semaZ2* expression in blue is apparent in r4. **C:** Dorsal view of 24 hpf embryo showing three clusters of *semaZ2* expressing cells (arrowheads) in the region of the pharyngeal arch primordia. **D:** Lateral view of pharyngeal arches at 36 hpf. Arrowheads denote *semaZ2* expressing cells in the arches. Expression is also strong in the developing fin bud (fb). **E:** Lateral view of pharyngeal arches at 48 hpf. Arrowheads denote *semaZ2* expression in the arches, and arrows denote *semaZ2* expression in the otocyst (oto). **F:** Ventral view of pharyngeal arches at 72 hpf. Arrowheads denote *semaZ2* expression. At this stage, *semaZ2* does not appear to be expressed in differentiated muscle (m) or cartilage (c). **G:** Lateral view of rostral trunk at 24 hpf showing small streams of *semaZ2* expressing cells medial to each somite in the position of migrating neural crest (arrowheads). **H:** Dorsal view of 27 hpf head showing *semaZ2* expression (arrowheads) at the medial surface of the nasal placodes (np). **I:** Lateral view of rostral trunk at 24 hpf. Migrating primordium of the posterior lateral line (mp) is outlined with dotted line. *semaZ2* is expressed in cells at the leading (caudal) half of the migrating primordium. **J:** Dorsal view of pectoral fin bud (fb) at 50 hpf showing strong *semaZ2* expression in the developing cartilage. **K:** Dorsal view of pectoral fin bud at 72 hpf showing more restricted *semaZ2* expression in distal cartilage. **L:** Lateral view of 24 hpf tail. *semaZ2* expression in notochord (noto) is limited to the caudal region at this age, and expression is also present in the tail bud (tb). Scale bars = 50 μm (A, E–K) and 100 μm (B–D, L).

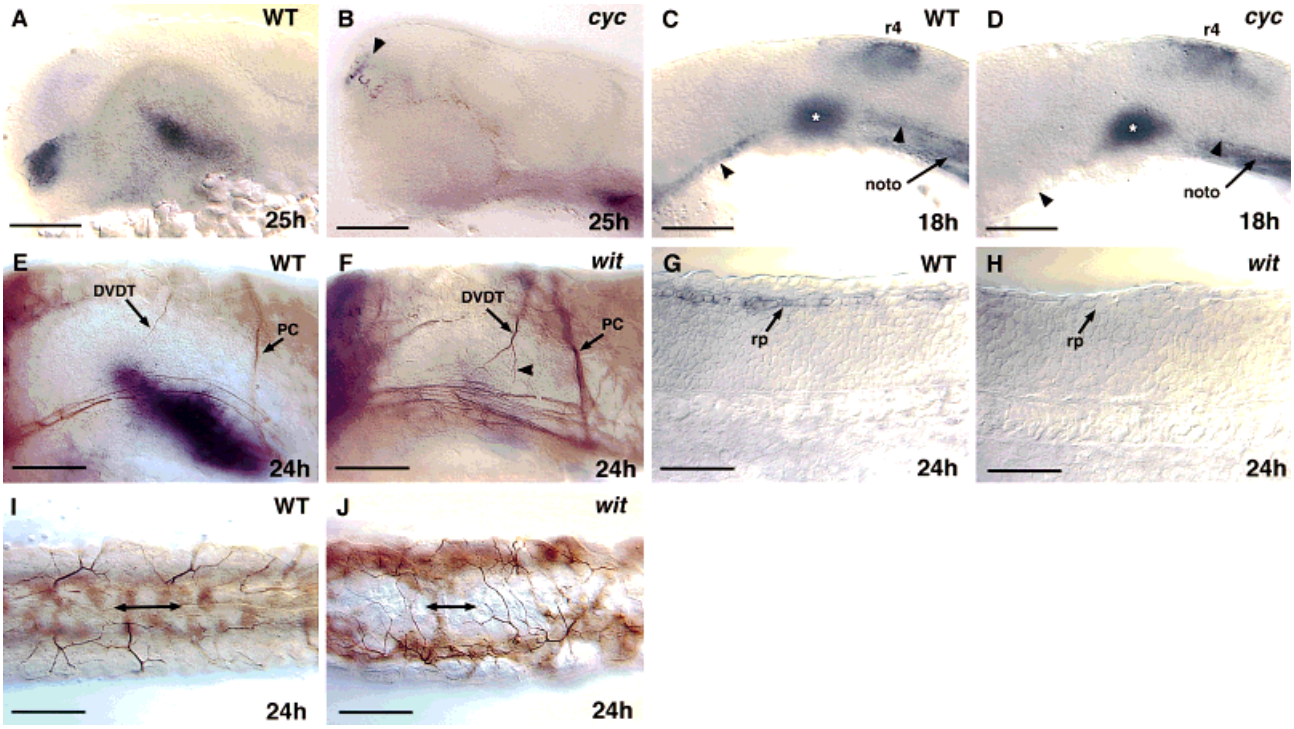

Fig. 4. Comparison of *semaZ2* expression and axon pathway formation in wild type and mutant embryos. **A,B:** Lateral views of 25 hpf head of wild-type embryo (A) and *cyc* embryo (B). The two domains of *semaZ2* expression in the diencephalon are absent in *cyc* embryos, although the normal expression in the nasal placode is present (arrowhead). **C,D:** Lateral views of 18 hpf wild type (C) and *cyc* (D) embryos showing *semaZ2* expression in the floor plate is present in wild-type but absent in *cyc* embryos (arrowheads). Expression in hindbrain rhombomeres, migrating neural crest (asterisk) and notochord is normal in *cyc*. r4, rhombomere 4. **E,F:** Lateral views of 24 hpf diencephalon in wild type (E) and *wit* (F) embryos with *semaZ2* mRNA expression in blue and axon pathways labeled with anti-tubulin in brown. *semaZ2* expression in the diencephalon is greatly reduced in *wit* embryos. Epiphysial axons extend ventrally in the DVDT and turn rostrally in the region of *semaZ2* expression in wild type (E). Epiphysial axons have aberrant caudal pathways in *wit* (arrowhead in F). **G,H:** Lateral views 24 hpf trunk in wild type (G) and *wit* (H) embryos showing *semaZ2* expression in the spinal cord roof plate (rp) is absent in *wit* mutants. **I,J:** Dorsal views of wild-type (I) and *wit* (J) trunk. Peripheral Rohon-Beard (RB) axons extending in skin are labeled with anti-tubulin in brown. Double arrows indicate dorsal midline. RB axons in wild-type embryos do not cross the dorsal midline (I), but do cross the midline in *wit* embryos (J). Scale bars = 100 μm (A–D), 50 μm (E–J).

zebrafish. Indeed, additional members of several gene families have been isolated in zebrafish and are hypothesized to be the result of chromosomal duplications during zebrafish evolution (Ekker et al., 1992; Akimenko et al.,1995; Prince et al.,1998).

As a first step toward understanding *semaZ2* function in vivo, we analyzed its developmental expression pattern. There are several regions of the developing zebrafish nervous system in which *semaZ2* is in a position both temporally and spatially to influence developing axon pathways. For example, *semaZ2* is expressed between the pathways of the epiphysial axons and the nucPC axons and could guide their growth cones to turn in opposite directions at the ventral diencephalon (Fig. 5A). Analysis of axon trajectories in the mutants *cyc* and *wit*, where *semaZ2* expression in the diencephalon is either completely missing or greatly reduced, supports the hypothesis that SemaZ2 normally contributes to the guidance of the epiphysial axons. The nucPC axons, however, do make their normal caudal turn in these mutants, and thus may be guided by additional cues. The increase in the incidence of caudally directed growth of the epiphysial axons in *cyc* and *wit* suggests the absence of a signal that normally prevents epiphysial growth cones from extending caudally (Fig. 5B). In addition, *cyc* embryos have an abnormal morphological crease in the diencephalon rostral to the epiphysial axons that may prevent them from making their normal rostral turn (Patel et al., 1994). However a mechanical barrier cannot account for the epiphysial pathfinding errors seen in *wit* embryos, because no crease or other abnormal structure is present in the diencephalon of *wit*. The *cyc* and *wit* mutations could also affect other potential guidance cues that may contribute to the observed axon trajectory errors. It is intriguing, however, that the correlation between reduced *semaZ2* expression and epiphysial axon errors is present in two separate mutants.

The expression of *semaZ2* by cells of the hindbrain floor plate may also reflect a role in guiding axons, and in particular guiding an axon's decision whether to cross the ventral midline. Numerous studies have

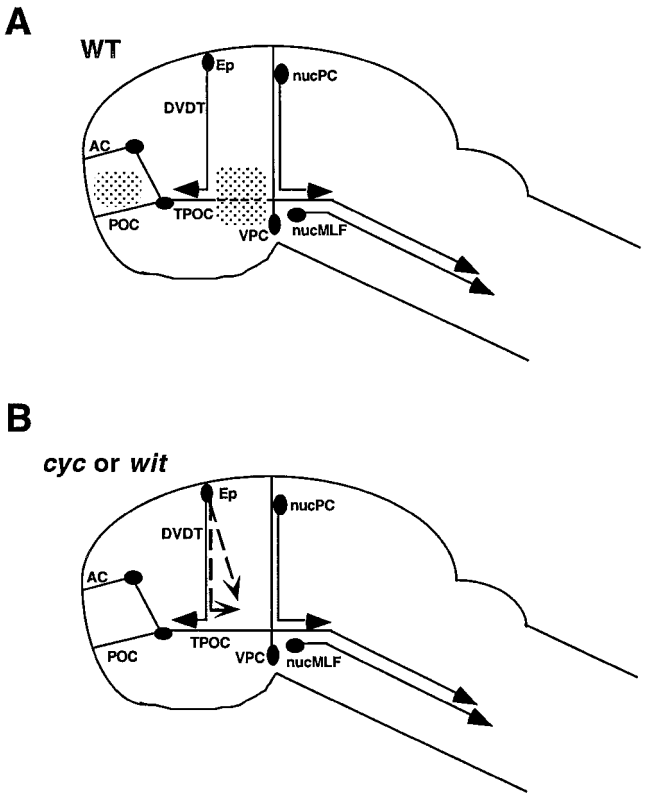

Fig. 5. Schematic representations of relationship between semaphorin expressing cells and developing axon pathways in wild type and mutant embryos. **A,B:** Schematics of lateral view of brain showing regions of *semaZ2* expression (stippled) and early axon tracts in wild-type (A) and *cyc* or *wit* (B). Black ovals represent clusters of cell bodies and black lines indicate axon pathways. Dotted arrows in (B) indicate epiphysial axon pathfinding errors seen in *cyc* and *wit* mutants. AC, anterior commissure; POC, post optic commissure; TPOC, tract of the post optic commissure; DVDT, dorsal ventral diencephalic tract; Ep, epiphisial neurons; nuc PC, nucleus of the posterior commissure; VPC, ventral nucleus of the posterior commissure; nucMLF, nucleus of the medial longitudinal fasciculus. **C,D:** Schematics of dorsal view of hindbrain in wild type (C) and *cyc* (D) embryos. Stippling indicates regions of the floor plate (FP) expressing *semaZ2*. Reticulospinal neurons are shown on one side only; however the same neurons are present on both sides of the hindbrain *in vivo*. Black circles indicate ipsilaterally projecting reticulospinal neurons, and open circles represent contralaterally projecting reticulospinal neurons (there are two contralaterally projecting neurons in rhombomere 6 in vivo). Dotted arc in (D) indicates reticulospinal pathfinding errors seen in *cyc*. oto, otocyst; r1–r6, rhombomeres 1–6.

demonstrated a role for the vertebrate floor plate in guiding axons at the ventral midline of the brain and spinal cord (Tessier-Lavigne et al., 1988; Placzek et al., 1990; Bovolenta and Dodd, 1991; Bernhardt et al., 1992a,b; Hatta, 1992; Shirasaki et al., 1995, 1996; Tamada et al., 1995). The floor plate has been shown to contain both attractive cues that signal axons to grow ventrally or to cross the midline (Tessier-Lavigne et al., 1988; Placzek et al., 1990; Shirasaki et al., 1995; Tamada et al., 1995), and repulsive cues that direct other axons away from the midline (Colamarino and Tessier-Lavigne, 1995; Guthrie and Pini, 1995; Tamada et al., 1995; Shirasaki et al., 1996). In some cases, the guidance molecules Netrin-1 or SemaD/III have been shown to mimic the attractive or repellant activity of floor plate (Kennedy et al., 1994; Serafini et al., 1994; Colamarino and Tessier-Lavigne, 1995; Varela-Echavarria et al., 1997). *netrin-1* is expressed in the floor plate at all axial levels, suggesting it has a general effect on axons throughout the neuraxis (Kennedy et al., 1994; Serafini et al., 1994; Lauderdale et al., 1997; Strähle et al., 1997). Indeed, floor plate from either brain or spinal cord has similar guidance effects on axons from explants of mesencephalon or metencephalon (Tamada et al., 1995). The *semaZ2* floor plate expression is particularly interesting because it is present in only a subset of floor plate cells in the hindbrain and midbrain for a limited developmental time period, and is never present in the spinal cord floor plate. It thus may have a highly specific effect on a subset of growing axons, perhaps modifying or fine tuning the effects of more generally expressed guidance cues. The hindbrain reticulospinal neurons, for instance, can be divided into seven classes based on whether their axons cross the midline and which longitudinal pathway they choose (Metcalfe et al., 1986). Each rhombomere contains a unique composition of these classes and may therefore require a unique combination of guidance cues to define their axonal pathways.

The expression pattern of *semaZ2* suggests it may also play a role in regulating axon pathway formation in the spinal cord. Although *semaZ2* is not expressed in the spinal cord floor plate, it is expressed in the notochord at the time when the first spinal axons are extending toward the ventral midline, and thus could potentially affect their pathfinding decisions at the ventral midline. In fact, the early spinal commissural growth cones cross the midline apposed to the basal lamina that lies between the spinal cord and notochord (Bernhardt et al., 1992a), and could therefore be affected by any cues secreted by the notochord into that basal lamina. When the notochord is laser ablated or absent as a result of the zebrafish *notail* mutation, growth cones of the spinal commissural axons make pathfinding errors at the ventral midline (Greenspoon et al., 1995), suggesting the notochord provides important cues signaling these growth cones to follow their appropriate pathways. It is possible that SemaZ2 secreted from the notochord may prevent particular classes of ipsilaterally projecting interneurons from crossing the ventral midline. For example, the ventral longitudinal descending (VeLD) axons are potentially responsive axons (Bernhardt et al., 1990; Kuwada et al., 1990a,b). These neurons lie in the ventral spinal cord and extend axons ventrally toward the floor plate. Upon reaching the midline region, the axons turn away from the floor plate and descend ipsilaterally, suggesting they may be repelled by a signal located at the midline.

SemaZ2 secreted from the spinal cord roof plate may play a role in guiding particular spinal axons to a ventral trajectory. A number of studies have indicated

that the attractive guidance molecule Netrin-1, expressed in the ventral spinal cord, functions to direct commissural axons toward the ventral midline in rodent and chick spinal cord (Kennedy et al., 1994; Serafini et al., 1994; 1996), as well as in zebrafish spinal cord (Lauderdale et al., 1997). Spinal commissural axons in *netrin-1* deficient mice begin their ventral trajectory normally, suggesting that Netrin-1 is not responsible for the growth cone's initial extension in the ventral direction (Serafini et al., 1996). Commissural axons may in fact be guided by a combination of repulsion away from the dorsal cord together with attraction toward the ventral cord. Experiments in which rat spinal cord roof plate is co-cultured with dorsal spinal cord explants containing commissural neurons show that a diffusible factor secreted from the roof plate inhibits commissural axon growth (Augsburger et al., 1996). SemaZ2 secreted from the roof plate may initially direct commissural axons to a ventral trajectory, like the role proposed for its potential homolog, chick Coll-2, which is expressed in the chick dorsal spinal cord (Luo et al., 1995). In zebrafish, SemaZ2 could act in concert with SemaZ7, a transmembrane semaphorin expressed in the dorsal spinal cord (Halloran et al., 1998). Because the expression of *semaZ2* in the spinal cord roof plate and of *semaZ7* in the dorsal cord appears after the very first commissural axons begin extending in the cord, these molecules are likely to affect only later extending axons, such as those of the secondary commissural ascending neurons or the commissural bifurcating neurons (Bernhardt et al., 1990).

Another potential role for SemaZ2 in the spinal cord roof plate is in guiding the peripheral axons of the sensory Rohon-Beard neurons. RB axons normally do not cross the dorsal midline, suggesting the presence of a guidance cue at the dorsal midline inhibitory to RB growth cones. In fact, *semaZ2* is expressed in the spinal cord roof plate during the time the RB axon abors are forming. Because the skin directly overlies the roof plate, SemaZ2 secreted from the roof plate is in a position to affect axons growing in the skin. In *wit* embryos, where *semaZ2* expression in the roof plate is undetectable, the RB axons are no longer restricted to the ipsilateral side. Instead, they readily grow over the dorsal midline, suggesting that SemaZ2 may normally act to prevent their growth across the dorsal midline.

EXPERIMENTAL PROCEDURES

Zebrafish

Zebrafish (*D. rerio*) were maintained in a laboratory breeding colony at 28.5°C on a 14 hr light/10 hr dark cycle. Embryos collected from the breeding fish were allowed to develop at 28.5°C and were staged as described by Kimmel et al. (1995). Embryo age is defined as hours post fertilization (hpf). The *cyclops*^{b16} mutation (Hatta et al., 1991) is a γ-ray induced mutation, and *whitetail*^{ta52b} (Jiang et al., 1996) is an ENU induced mutation.

Isolation of cDNA clones

To isolate *semaZ2*, a 16–20 hpf zebrafish λgt10 cDNA library was initially screened with a chick *collapsin-1* probe under low stringency conditions (55°C, 6×SSC). Weakly hybridizing plaques then were rescreened and purified using a *semaZ1a* fragment as a probe (55°C, 2×SSC). A 1.8 kb cDNA was isolated and subcloned into pBluescript SK-. Both strands of the cDNA insert were sequenced with T7 DNA polymerase (Sequenase 2.0 sequencing kit, Amersham, Arlington Heights, IL). This cDNA encoded a partial semaphorin lacking the 5' region of the gene. To search for a full length *semaZ2* cDNA, the λgt10 library was rescreened under high stringency conditions (65°C, 0.1×SSC) by using a portion of the *semaZ2* sema domain as a probe. This screen yielded a longer *semaZ2* cDNA that was still lacking the translation initiation site. Rapid amplification of cDNA ends (5' RACE, Gibco-BRL, Gaithersburg, MD) was then used to synthesize the 5' end. RACE products from three independent PCR reactions were subcloned into pBluescript SK- and sequenced. A complete *semaZ2* cDNA was generated by ligating the RACE cDNA fragment to the cDNA obtained from the λgt10 library screen.

Sequence analyses of cDNAs was carried out with the MacVector software package (Kodak Scientific Imaging Systems, Rochester, NY), and the Genetics Computer Group (GCG) Wisconsin package Version 9.1. Comparisons of the amino acid identity between semaphorins was carried out with the GCG FASTA and GAP programs. The predicted signal peptide cleavage site was determined based on the rules of von Heijne (1986).

PCR

PCR was performed on cDNA reverse transcribed from 24 hpf zebrafish total RNA. Primers used were fully degenerate and encoded the first 23 bases of the sequence KWTTFLKA and DPYCAWD. The primers were annealed to the template at 45°C for 1 min and extended at 74°C for 1 min, for 35 cycles. PCR products were subcloned into the pCR-II vector with the TA cloning kit (Invitrogen, La Jolla, CA), and the resulting inserts sequenced.

Whole Mount In Situ Hybridization and Immunohistochemistry

Riboprobes labeled with digoxygenin-UTP were synthesized by in vitro transcription and hydrolyzed to an average length of 200–500 bases by limited alkaline hydrolysis (Cox et al., 1994). Whole mount in situ hybridization was performed as described by Schulte-Merker et al. (1992), except the acetic anhydride/triethanolamine treatment was omitted, and hybridizations were carried out at 65°C. For the two color in situ hybridization with *semaZ2* and *krox20*, FITC-labeled antisense riboprobes to *krox20* were synthesized, and hybridization with both probes was carried out simultaneously. After completion of the coloration reaction for

semaZ2, the alkaline phosphatase was heat inactivated (65°C, 1 hr) and embryos placed in anti-FITC antibody conjugated to alkaline phosphatase (Boehringer-Mannheim, Mannheim, Germany) overnight. The *krox20* color was developed with Fast Red TR/Naphthol AS-MX (Sigma Chemical Company, St. Louis, MO, F4648). Embryos were mounted in 70% glycerol.

For double-labeling with in situ hybridization and anti-tubulin, the monoclonal antibody for acetylated α-tubulin (Sigma, T6793) was added to the anti-digoxygenin antibody during the in situ hybridization. After the in situ color reaction was complete, embryos were fixed in 4% paraformaldehyde overnight. Anti-tubulin labeling was then completed with the Vectastain Mouse IgG ABC immunoperoxidase labeling kit (Vector Labs, Burlingame, CA).

Sections were made with a cryostat after whole mount in situ hybridization. Embryos were equilibrated in 30% sucrose, embedded in OCT compound (Miles, Elkhart, IN), and cut into 16 μm sections on a cryostat. Sections were mounted in 70% glycerol.

ACKNOWLEDGMENTS

We thank Dr. Nadean Brown, Dr. Anand Chandrasekhar, Dr. James Lauderdale, Dr. Wataru Shoji, and Dr. James Warren for many helpful discussions during this study. We also thank Dr. Hitoshi Okamoto for the gift of the cDNA library, Dr. Trevor Jowett for the *krox20* clone, Dr. Charles B. Kimmel for *cyclops* mutant fish, Dr. Christiane Nüsslein-Volhard, and Dr. Hans-Georg Frohnhöfer for *whitetail* mutants. Thanks to Dr. Marc Roos, Dr. Robert Bernhardt, and Dr. Melitta Schachner for sharing unpublished results. Special thanks to Dr. Fengyun Su for supervision of our zebrafish colony. Molecular analysis was supported by an NIH grant (M01RR00042) to the General Clinical Research Center at the University of Michigan. This work was supported by an NRSA postdoctoral fellowship (NS09877–01) to M.C.H., and grants from NINDS (NS36587) and APA (KAI-9603 and KAR1–9704) to J.Y.K.

REFERENCES

Adams RH, Betz H, Püschel AW. 1996. A novel class of murine semaphorins with homology to thrombospondin is differentially expressed during early embryogenesis. Mech Dev 57:33–45.

Akimenko M-A, Johnson SL, Westerfield M, Ekker M. 1995. Differential induction of four *msx* homeobox genes during fin development and regeneration in zebrafish. Development 121:347–357.

Augsburger A, Schuchardt A, Hoskins S, Dodd J. 1996. Repulsion of spinal commissural axons by a diffusible factor from the roof plate. Soc Neurosci Abstr 22:1473.

Behar O, Golden JA, MashimoH, Schoen FJ, Fishman M.C. 1996. Semaphorin III is needed for normal patterning and growth of nerves, bones and heart. Nature 383:525–528.

Bernhardt RR, Chitnis AB, Lindamer L, Kuwada JY. 1990. Identification of spinal neurons in the embryonic and larval zebrafish. J Comp Neurol 302:603–616.

Bernhardt RR, Nguyen N, Kuwada, JY. 1992a. Growth cone guidance by floor plate cells in the spinal cord of zebrafish embryos. Neuron 8:869–882.

Bernhardt RR, Patel CK, Wilson SW, Kuwada JY. 1992b. Axonal trajectories and distribution of GABAergic spinal neurons in wild-type and mutant zebrafish lacking floor plate cells. J Comp Neurol 326:263–272.

Bovolenta P, Dodd J. 1991. Perturbation of neuronal differentiation and axon guidance in the spinal cord of mouse embryos lacking a floor plate: analysis of Danforth's short-tail mutation. Development 113:625–639.

Chitnis AB, Kuwada JY. 1990. Axonogenesis in the brain of zebrafish embryos. J Neurosci 10:1892–1905.

Christensen CR, Klingelhofer J, Tarabykina S, Hulgaard EF, Kramerov D, Lukanidin E. 1998. Transcription of a novel mouse semaphorin gene, M-semaH, correlates with the metastatic ability of mouse tumor cell lines. Cancer Res 58:1238–1244.

Colamarino SA, Tessier-Lavigne M. 1995. The axonal chemoattractant netrin-1 is also a chemorepellent for trochlear motor axons. Cell 81:621–629.

Cox KH, DeLeon DV, Angerer LM, Angerer RC. 1994. Detection of mRNAs in sea urchin embryos by *in situ* hybridization using asymmetric RNA probes. Dev Biol 101:485–502.

Culotti, JG, Kolodkin, AL. 1996. Functions of netrins and semaphorins in axon guidance. Curr Opin Neurobiol 6:81–88.

Eckhardt F, Behar O, Calautti E, Yonezawa K, Nishimoto I, Fishman MC. 1997. A novel transmembrane semaphorin can bind *c-src*. Mol Cell Neurosci 9:409–419.

Eisen JS, Myers PZ, Westerfield M. 1986. Pathway selection by growth cones of identified motoneurones in live zebra fish embryos. Nature 320:269–271.

Ekker M, Wegner J, Akimenko MA, Westerfield M. 1992. Coordinate expression of three *engrailed* genes. Development 116:1001–1012.

Furuyama T, Inagaki S, Kosugi A, Noda S, Saitoh S, Ogata M, Iwahashi Y, Miyazaki N, Hamaoka T, Tohyama M. 1996. Identification of a novel transmembrane semaphorin expressed on lymphocytes. J Biol Chem 271:33376–33381.

Giger RJ, Wolfer DP, De Wit GMJ, Verhaagen J 1996. Anatomy of rat *semaphorin III/collapsin-1* mRNA expression and relationship to developing nerve tracts during neuroembryogenesis. J Comp Neurol 375:378–392.

Greenspoon S, Patel CK, Hashmi S, Bernhardt RR. Kuwada JY. 1995. The notochord and floor plate guide growth cones in the zebrafish spinal cord. J Neurosci 15:5956–5965.

Guthrie S, Pini A. 1995. Chemorepulsion of developing motor axons by the floor plate. Neuron 14:1117–1130.

Hall KT Boumsell L, Schultze JL, Boussiotis VA, Dorfman DM, Cardoso AA, Bensussan A, Nadler LM, Freeman GJ. 1996. Human CD100, a novel leukocyte semaphorin that promotes B-cell aggregation and differentiation. Proc Natl Acad Sci USA 93:11780–11785.

Halloran MC, Severance SM, Yee CS, Gemza DL, Kuwada JY. 1998. Molecular cloning and expression of two novel zebrafish semaphorins. Mech Dev 76:165–168.

Hatta K, Kimmel CB, Ho RK, Walker C. 1991. The *cyclops* mutation blocks specification of the floor plate of the zebrafish central nervous system. Nature 350:339–341.

Hatta K. 1992. Role of the floor plate in axonal patterning in the zebrafish CNS. Neuron 9:629–642.

Inagaki S, Furuyama T, Iwahashi Y. 1995. Identification of a member of mouse semaphorin family. Febs Lett 370:269–272.

Jiang Y.-J, Brand M, Heisenberg C.-P, Beuchle D, Furutani-Seiki M, Kelsh RN, Warga RM, Granato M, Haffter P, Hammerschmidt M, Kane DA, Mullins MC, Odenthal J, van Eeden FJM, Nüsslein-Volhard C. 1996. Mutations affecting neurogenesis and brain morphology in the zebrafish, Danio rerio. Development 123:205–216.

Kennedy TE, Serafini T, de la Torre JR, Tessier-Lavigne M. 1994. Netrins are diffusible chemotropic factors for commissural axons in the embryonic spinal cord. Cell 78:425–435.

Kikuchi K, Ishida H, Kimura, T. 1997. Molecular cloning of a novel member of semaphorin family genes, semaphorin Z. Brain Res Mol Brain Res 51:229–237.

Kimmel CB, Ballard WW, Kimmel SR, Ullmann B, Schilling TF. 1995. Stages of embryonic development of the zebrafish. Dev Dyn 203:253–310.

Kobayashi H, Koppel AM, Luo Y, Raper JA. 1997. A role for collapsin-1 in olfactory and cranial sensory axon guidance. J Neurosci 17:8339–8352.

Kolodkin AL. 1996. Growth cones and the cues that repel them. Trends Neurosci 19:507–513.

Kolodkin AL, Matthes DJ, O'Connor TP, Patel NH, Admon A, Bentley D, Goodman CS. 1992. Fasciclin IV: sequence, expression, and function during growth cone guidance in the grasshopper embryo. Neuron 9:831–845.

Kolodkin AL, Matthes DJ, Goodman CS. 1993. The semaphorin genes encode a family of transmembrane and secreted growth cone guidance molecules. Cell 75:1389–1399.

Kuwada JY, Bernhardt RR, Chitnis, AB. 1990a. Pathfinding by identified growth cones in the spinal cord of zebrafish embryos. J Neurosci 10:1299–1308.

Kuwada JY, Bernhardt RR, Nguyen N. 1990b. Development of spinal neurons and tracts in the zebrafish embryo. J Comp Neurol 302:617–628.

Lauderdale JD, Davis NM, Kuwada JY. 1997. Axon tracts correlate with *netrin-1a* expression in the zebrafish embryo. Mol Cell Neurosci 9:293–313.

Luo Y, Raible D, Raper, JA. 1993. Collapsin, a protein in brain that induces the collapse and paralysis of neuronal growth cones. Cell 75:217–227.

Luo Y, Shepherd I, Li J, Renzi MJ, Chang S, Raper, JA. 1995. A family of molecules related to collapsin in the embryonic chick nervous system. Neuron 14:1131–1140.

Matthes DJ, Sink H, Kolodkin AL, Goodman CS. 1995. Semaphorin II can function as a selective inhibitor of specific synaptic arborizations. Cell 81:631–639.

Mendelson B. 1986. Development of reticulospinal neurons of the zebrafish. II. Early axonal outgrowth and cell body position. J Comp Neurol 251:172–184.

Messersmith EK, Leonardo ED, Shatz CJ, Tessier-Lavigne M, Goodman CS, Kolodkin AL. 1995. Semaphorin III can function as a selective chemorepellent to pattern sensory projections in the spinal cord. Neuron 14:949–959.

Metcalfe WK, Mendelson B, Kimmel CB. 1986. Segmental homologies among reticulospinal neurons in the hindbrain of the zebrafish larva. J Comp Neurol 251:147–159.

Myers PZ, Eisen JS, Westerfield M. 1986. Development and axonal outgrowth of identified motoneurons in the zebrafish. J Neurosci 6:2278–2289.

Oxtoby E, Jowett T. 1993. Cloning of the zebrafish *krox-20* gene (*krx-20* and its expression during hindbrain development. Nucleic Acids Res 21:1087–1095.

Patel CK, Rodriguez LC, Kuwada JY. 1994. Axonal outgrowth within the abnormal scaffold of brain tracts in a zebrafish mutant. J Neurobiol 25:345–360.

Placzek M, Tessier-Lavigne M, Jessell T, Dodd J. 1990. Orientation of commissural axons in vitro in response to a floor plate- derived chemoattractant. Development 110:19–30.

Püschel AW, Adams RH, Betz H. 1995. Murine *semaphorin D/collapsin* is a member of a diverse gene family and creates domains inhibitory for axonal extension. Neuron 14:941–948.

Püschel AW, Adams RH, Betz H. 1996. The sensory innervation of the mouse spinal cord may be patterned by differential expression of and differential responsiveness to semaphorins. Mol Cell Neurosci 7:419–431.

Prince VE, Joly L, Ekker M, Ho RK. 1998. Zebrafish hox genes: genomic organization and modified colinear expression patterns in the trunk. Development 125:407–420.

Roche J, Boldog F, Robinson M, Robinson L, Varella GM, Swanton M, Waggoner B, Fishel R, Franklin W, Gemmill R, Drabkin H. 1996. Distinct 3p21.3 deletions in lung cancer and identification of a new human semaphorin. Oncogene 12:1289–1297.

Ross LS, Parrett, T, Easter SJ. 1992. Axonogenesis and morphogenesis in the embryonic zebrafish brain. J Neurosci 12:467–482.

Schilling TF. Kimmel CB. 1994. Segment and cell type lineage restrictions during pharyngeal arch development in the zebrafish embryo. Development 120:483–494.

Schulte-Merker S, Ho RK, Herrmann BG. Nüsslein-Volhard C. 1992. The protein product of the zebrafish homologue of the mouse T gene is expressed in nuclei of the germ ring and the notochord of the early embryo. Development 116:1021–1032.

Sekido Y, Bader S, Latif F, Chen JY, Duh FM, Wei MH, Albanesi JP, Lee CC, Lerman MI, Minna JD. 1996. Human semaphorins A(V) and IV reside in the 3p21.3 small cell lung cancer deletion region and demonstrate distinct expression patterns. Proc Natl Acad Sci USA 93:4120–4125.

Serafini T, Kennedy TE, Galko MJ, Mirzayan C, Jessell TM, Tessier-Lavigne M. 1994. The netrins define a family of axon outgrowth-promoting proteins homologous to C. elegans UNC-6. Cell 78:409–424.

Serafini T, Colamarino SA, Leonardo ED, Wang H, Beddington R, Skarnes WC, Tessier-Lavigne M. 1996. Netrin-1 is required for commissural axon guidance in the developing vertebrate nervous system. Cell 87:1001–1014.

Shepherd IT, Luo Y, Lefcort F, Reichardt LF, Raper JA. 1997. A sensory axon repellent secreted from ventral spinal cord explants is neutralized by antibodies raised against collapsin-1. Development 124:1377–1385.

Shirasaki R, Tamada A, Katsumata R, Murakami, F. 1995. Guidance of cerebellofugal axons in the rat embryo: directed growth toward the floor plate and subsequent elongation along the longitudinal axis. Neuron 14:961–972.

Shirasaki R, Mirzayan C, Tessier-Lavigne M, Murakami F. 1996. Guidance of circumferentially growing axons by netrin-dependent and - independent floor plate chemotropism in the vertebrate brain. Neuron 17:1079–1088.

Shoji W, Yee C, Kuwada J. 1998. Zebrafish Semaphorin Z1a collapses specific growth cones and alters their pathway *in vivo*. Development 125:1275–1283.

Strähle U, Fischer N, Blader P. 1997. Expression and regulation of a *netrin* homologue in the zebrafish embryo. Mech Dev 62:147–160.

Tamada A, Shirasaki R, Murakami F. 1995. Floor plate chemoattracts crossed axons and chemorepels uncrossed axons in the vertebrate brain. Neuron 14:1083–1093.

Taniguchi M, Yuasa S, Fujisawa H, Naruse I, Saga S, Mishina M, Yagi T. 1997. Disruption of *semaphorin III/D* gene causes severe abnormality in peripheral nerve projection. Neuron 19:519–530.

Tessier-Lavigne M, Placzek M, Lumsden AG, Dodd J. Jessell TM. 1988. Chemotropic guidance of developing axons in the mammalian central nervous system. Nature 336:775–778.

Tessier-Lavigne M, Goodman CS. 1996. The molecular biology of axon guidance. Science 274:1123–1133.

Tevarrow B, Marks DL, Kimmel CB. 1990. Organization of hindbrain segments in the zebrafish embryo. Neuron 4:669–679.

Varela-Echavarria A, Tucker A, Püschel AW, Guthrie S. 1997. Motor axon subpopulations respond differentially to the chemorepellents netrin-1 and semaphorin D. Neuron 18:193–207.

von Heijne G. 1986. A new method for predicting signal sequence cleavage sites. Nucleic Acids Res. 14:4683–4690

Wilson SW, Ross LS, Parrett T, Easter SJ. 1990. The development of a simple scaffold of axon tracts in the brain of the embryonic zebrafish, *Brachydanio rerio*. Development 108:121–145.

Winberg ML, Mitchell KJ, Goodman CS. 1998. Genetic analysis of the mechanisms controlling target selection: complementary and combinatorial functions of netrins, semaphorins, and IgCAMs. Cell 93:581–591.

Wong J, Yu W, Connor T. 1997. Transmembrane grasshopper Semaphorin I promotes axon outgrowth *in vivo*. Development 124:3597–3607.

Xiang RH, Hensel CH, Garcia DK, Carlson HC, Kok K, Daly MC, Kerbacher K, van den Berg A, Veldhuis P, Buys CH, Naylor SL. 1996. Isolation of the human *semaphorin III/F* gene (SEMA3F) at chromosome 3p21, a region deleted in lung cancer. Genomics 32:39–48.

Yee CS, Chandrasekhar A, Kuwada JY. 1995. Molecular cloning and analysis of a zebrafish collapsin. Soc Neurosci Abstr 21:124.14.

Yu HH, Araj HH, Ralls SA, Kolodkin AL. 1998. The transmembrane Semaphorin Sema I is required in *Drosophila* for embryonic motor and CNS axon guidance. Neuron 20:207–220.

Zhou L, White FA, Lentz SI, Wright DE, Fisher DA, Snider WD. 1997. Cloning and expression of a novel murine *semaphorin* with structural similarity to insect *semaphorin I*. Mol Cell Neurosci 9:26–41.